

PAPER • OPEN ACCESS

Hydrogen contamination in liquid helium

To cite this article: J Will and C Haberstroh 2020 *IOP Conf. Ser.: Mater. Sci. Eng.* **755** 012117

View the [article online](#) for updates and enhancements.

You may also like

- [Thermal Effects in High Compactness CEA Stack](#)
Manon Elie, DI Iorio Stephane, Thomas Carlioz et al.
- [Solid Dispersion Flow Battery Particle Synthesis and Electrochemical Characterization](#)
Gary Koenig
- [CFD Simulation of Multistack Solid Oxide Cell Module Systems](#)
Ali Shahanaghi and Matti Noponen

Hydrogen contamination in liquid helium

J Will and C Haberstroh

Bitzer Chair of Refrigeration, Cryogenics and Compressor Technology,
Technische Universitaet Dresden, 01062 Dresden, Germany

julian.will@tu-dresden.de

Abstract. For some years now, massive problems are often occurring when operating standard flow cryostats with pumped liquid helium. There are a large number of reports from various parts of the world, describing blockage problems arising typically within a few hours. Standard equipment for measuring material properties at temperatures below 4.2 K is massively affected. Hydrogen contamination within the used liquid helium could be identified as direct cause. With helium evaporating in the narrow throttling passages, hydrogen in solid state accumulates and is forming blockages. Usually internal capillaries or inlet valves are concerned. In consequence, the helium flow is reduced or ceasing completely, the operating temperature of the cryostat can't be upheld, and the measurement run must be interrupted. Extremely low concentrations in the sub-ppm range are sufficient to block the helium flow within a few hours of operation. This contribution contains first quantifications regarding these contamination. A semi-quantitative analysis method using a narrow flow resistor, as well as gas chromatographic investigations led to new findings. Effects within the liquid helium supply that give rise to the problem were scrutinized. The collected results should lead to an understanding and to feasible solutions of the problem.

Keywords. Liquid helium, Hydrogen contamination, Flow cryostat, Blockage of capillaries, Blockage of valves, Solubility of hydrogen in liquid helium

1. Introduction

Liquid helium is used in cryogenic laboratories worldwide. Here, for example, it is utilized in cryostats to measure physical properties at low temperatures. At normal pressure liquid helium has a saturation temperature of $T_{s\ He} = 4.2\ K$. If lower temperatures are required, this can be achieved by pressure reduction. For this purpose, cryostat internal narrow throttling passages (capillaries) or throttling valves are used. During the through-flow the pressure of the helium is lowered, the saturation temperature decreases accordingly and evaporative cooling down to $T < 1.8\ K$ can be realized. Blockage problems have been occurring at this point for several years now. Hydrogen precipitates in solid form during the helium evaporation and accumulates at the throttle location. Figure 1 illustrates the principle of such a cryostat and of the blockage formation. Depending on the operation parameters, this leads to a blockage of the capillary or the valve after a few hours. As early as 2005, German helium users addressed this issue to our chair. In the meantime, a large number of cases have been reported in Europe. Ikeda et al. [1] report from affected institutes in Asia and refer to hydrogen as the cause. Optimizations of the internal adsorption purifier of a small existing liquefaction plant were presented as a remedial attempt. In 2014, Decker et al. [2] considered the existence of neon and hydrogen as possible impurities in a redesign of the internal purification system of liquefiers.



Most of the literature is published by the Spanish University of Zaragoza. The PhD thesis of Dr. Miguel Gabal Lanau [3] describes the development of a cryocondensation purifier for helium gas, together with the company Quantum Design. However, the separation of hydrogen by this system is based on the use of getter materials. For the first time, Gabal et al. ([4], [5], [6] and [7]) describe the blockage effect, demonstrate the detection of hydrogen in liquid helium with a detection tool that uses a strong flow resistor. Furthermore, the cryocondensation purifier in connection with cryocooler-based small helium liquefier was introduced.

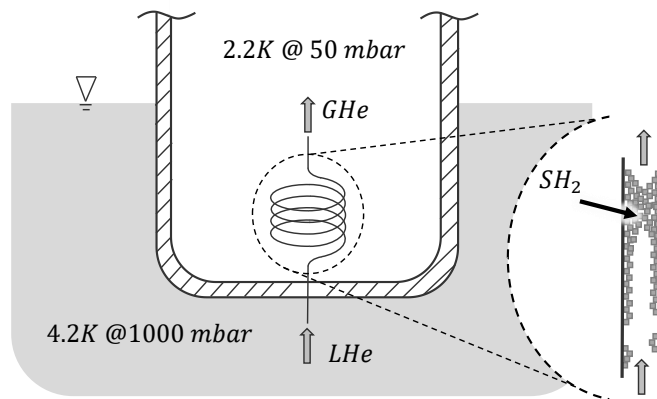


Figure 1. Through a narrow throttling passage (capillary) liquid helium (*LHe*) is driven into a vacuum chamber. Due to the pressure reduction the helium evaporates and a temperature of e.g. 2.2 K at ≈ 50 mbar is reached in the chamber. Within the capillary, hydrogen separates from the two phase helium flow and accumulates as a solid phase (*SH₂*) on the inner walls. This creates a solid, clogging block and the function of the cryostat fails.

In the present work, it is first verified whether hydrogen is plausible as a cause. A macroscopic model is presented which should provide an understanding of the helium/hydrogen system. A calculation of solubility is introduced, as well as the related challenges. A quantification of the hydrogen contamination is achieved by gas chromatographic measurements. Exemplary results for the detection of hydrogen, generated with the mentioned detection tool of the University of Zaragoza, are shown.

2. Plausibility of hydrogen as direct cause

The question arises whether hydrogen impurities are clearly the reason for the observed phenomena. A strong indication for this is that a blockage that has occurred can be eliminated by warming up the affected throttling location to $T = 20 \dots 30$ K. The melting and evaporation line of hydrogen begins at $T_{t H_2} \approx 14$ K (triple point). This fits to the observed dissolution of a solid hydrogen accumulation in the mentioned temperature range. Another conceivable contamination which could have a similar behaviour in said temperature range is neon ($T_{t Ne} \approx 24.5$ K). However, Gabal et al. were able to show by the controlled initiation and dissolution of a blockage under laboratory conditions that the dissolution takes place at a temperature just above the triple point of hydrogen ([3], [4]). Moreover, a peak at mass number 2 could be detected mass spectrometrically at the moment of blockage dissolution in the off-gas stream. Neon can therefore be excluded as primary cause. In addition, it must be checked whether the observed blockage times are plausible. In everyday laboratory work, total blockages occur after one to a few hours. A simple calculation approach is used for the plausibility check. A common capillary diameter is $66 \mu\text{m}$. The inner helium stream transports hydrogen, which separates at the inner walls of the capillary. It is the time to be calculated that is needed to build a solid hydrogen cylinder that height is twice the diameter (Figure 2, left). The required time is a function of the helium volume flow and the hydrogen concentration contained. The diagram in Figure 2 shows the calculated results. The duration of a full blockage Δt in function of the helium volume flow \dot{V}_{GHe} is given. The time frame of the blockage duration in the affected institutes is also shown. Three cases are plotted, based on the measurements achieved so far (see sections 3 and 4). It is assumed that all present hydrogen freezes out and thus serves to establish the blockage cylinder. The three cases cover the measured contents $x_{H_2} = 440 \text{ ppb}_{vol}$, $x_{H_2} = 200 \text{ ppb}_{vol}$ and $x_{H_2} = 130 \text{ ppb}_{vol}$ (ppb_{vol} : volumetric parts per billion, $\times 10^{-9}$).

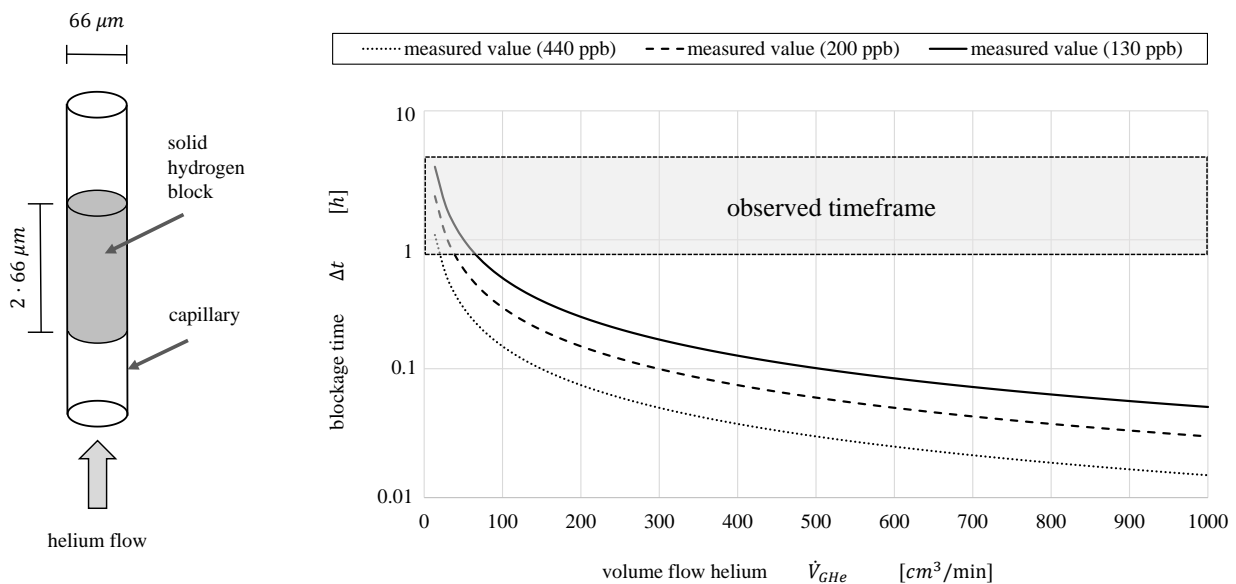


Figure 2. Left: Scheme of the blockage build up. In the capillary through which the helium flow passes, all hydrogen contamination will freeze out and form a cylindrical solid block. Right: The diagram shows the results based on a simple calculation model. The curves show the duration of the blockage build up.

It can be seen that the calculated blockages over a wide volume flow range do not overlap with the observed timeframe, but occur much faster. In fact, it becomes clear that extremely small amounts of hydrogen are capable of forming a suitable block. If only 10 % of the measured hydrogen quantity participates in the blockage, the model would provide the observed times.

3. System Helium/Hydrogen

For understanding of the helium/hydrogen phenomena here, a model was figured out. According to the model, liquid helium contains both dissolved and crystalline hydrogen. Measured values exist, which give the scales to be expected. Furthermore, the results of a calculation method are presented.

3.1. Macroscopic model

A macroscopic perspective of the behaviour of hydrogen contamination in liquid helium is adequate. Figure 3 illustrates a helium reservoir contaminated with hydrogen under normal pressure. It is subject to gravity and a stable temperature stratification is established. The reservoir consists of a liquid phase at the bottom and a gas phase above. Moreover, it is divided into three different temperature ranges. The upper range starts at any temperature $T > T_{tH_2}$ and extends to the triple point temperature of hydrogen ($T_{tH_2} = 14\text{ K}$). A simple gas mixture is present in this area.

The second range starts at the triple point temperature of the hydrogen and ends at the surface of the liquid helium at saturation temperature ($T_{sHe} = 4.2\text{ K}$). In this range, macroscopic quantities of hydrogen strive to become solid. Smallest crystals are formed together with other near molecules. If these find their way to the liquid helium surface, these adhere to the surface and can form floating accumulations together with other crystals. Solid hydrogen with a density of $\rho_{SH_2} = 86\text{ kg/m}^3$ [8] is the only solid with a lower density than liquid helium ($\rho_{LHe} = 125\text{ kg/m}^3$) [9]. An experiment carried out by the University of Zaragoza shows the formation of floating hydrogen “boats”. It can be presumed that hydrogen molecules are also striving to remain in this cold region due to the higher density.

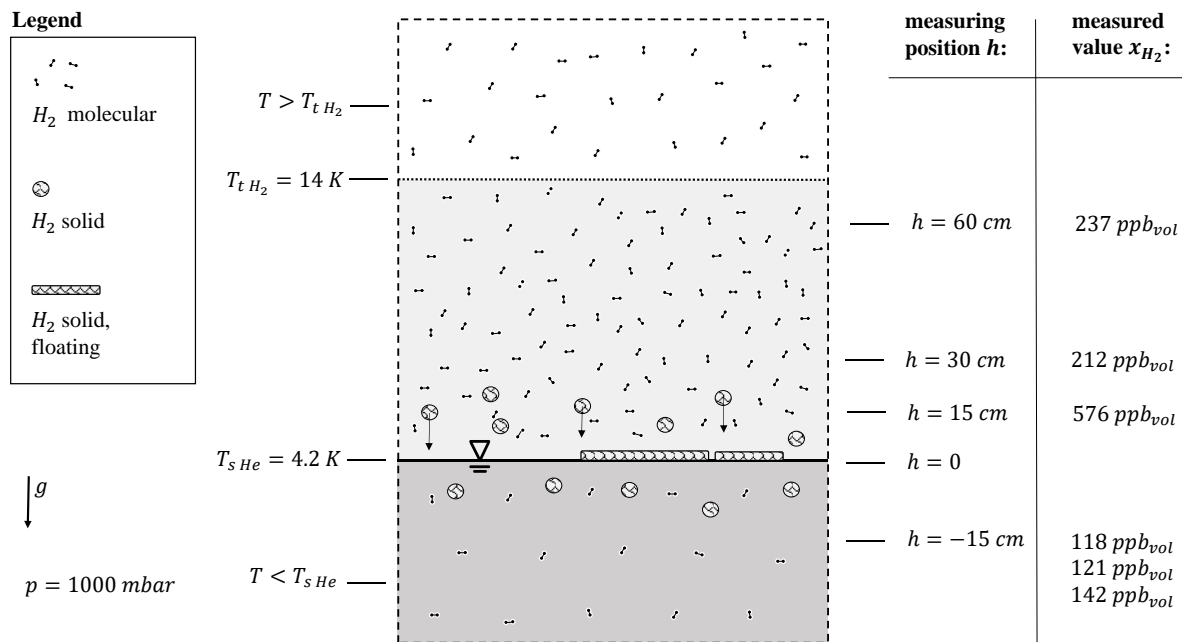


Figure 3. Model for the visualization of the macroscopic system helium/hydrogen. The model is divided into three temperature ranges in which the hydrogen behaves differently. Gas chromatographic analyses in various positions of the vertical axis support the concept.

The third region represents the liquid helium at $T_{LHe} \leq 4.2 \text{ K}$. Hydrogen exists in a dissolved state and in a solid crystalline state. These smallest crystals originate from the hydrogen adhering to the phase boundary.

3.2. Gas chromatographic analysis on a transport dewar

A critically contaminated liquid helium filling from a 100 liter transport dewar was analysed by gas chromatography at various points. The helium was liquefied from the liquefier operated by the university.

The results are also shown in Figure 3. In the cold gas phase ($T < T_{t H_2}$), values slightly higher 200 ppb_{vol} have been found. These two measurements at a height of 60 cm and respectively 30 cm above the phase boundary show the same range. In the cold gas near the phase boundary ($h = 15 \text{ cm}$), there is an increase in concentration. A value of $x_{H_2} = 576 \text{ ppb}_{vol}$ was measured here. This is a good indication that hydrogen is "captured" in the very cold region. A particularly high concentration directly at the phase boundary (due to floating solid hydrogen) has not yet been verified. Three measurements were carried out in the liquid phase. These also are in a stable range. The values $x_{H_2} = 118 \text{ ppb}_{vol}$, $x_{H_2} = 121 \text{ ppb}_{vol}$ and $x_{H_2} = 142 \text{ ppb}_{vol}$ were found ($\bar{x}_{H_2} = 130 \text{ ppb}_{vol}$).

The values give an idea of the actual contamination magnitude. They cannot be interpreted as a solubility limit. For this it is necessary to exclude the possible presence of crystalline hydrogen in the liquid. Furthermore, the calibration of the detectors in this value range must be closely examined. Different calibration standards from institute to institute cause different interpretations of the contents. This is particularly problematic in the analysis of trace gases, such as in this case. Measurements (section 4) on a liquid phase with a different standard yielded values of $x_{H_2} = 200 \text{ ppb}_{vol}$ and $x_{H_2} = 440 \text{ ppb}_{vol}$.

3.3. Calculation of solubility limit

Probably, dissolved and crystalline hydrogen can coexist in liquid helium and are extremely hard to distinguish. A calculation of the solubility limit is a first step in estimating the proportions. The Regular Solution Theory (RST) is used for this purpose. It is based on the equilibrium of the chemical potentials of the different phases of a component in the solvent at constant temperature ([10], [11]):

$$\ln x_i^L = -\frac{\Delta H_{f,m,i}(T_{f,i})}{RT} \left(1 - \frac{T}{T_{f,i}}\right) - \frac{\Delta c_{p,m,i}^{S \rightarrow L}}{R} \left(1 - \frac{T_{f,i}}{T}\right) + \frac{\Delta c_{p,m,i}^{S \rightarrow L}}{R} \ln \frac{T}{T_{f,i}} - \ln \gamma_i^L \quad (1)$$

The concentration content x of a component i in the solubility equilibrium is primarily dependent on the molar heat of fusion of the substance at the melting point $\Delta H_{f,m,i}(T_{f,i})$. This first term describes the *ideal solubility* behavior. The calculation can now be extended by the change of the heat capacity between solid and liquid state $\Delta c_{p,m,i}^{S \rightarrow L}$. The term, depending on the activity coefficient γ_i^L , completes the calculation method. The activity coefficient includes the interaction between the molecules. Prausnitz et al. [11] describe the calculation of the activity coefficient by means of the solubility parameter δ . This provides a good estimate of the behavior of non-polar atomic bonds, formula (2).

$$RT \cdot \ln \gamma_i^L = V_{m,i}^L \phi_j^2 [(\delta_i - \delta_j)^2 + 2l_{ij}\delta_i\delta_j] \quad (2)$$

The equation is further dependent on the molar volume of the solute $V_{m,i}^L$ and the volume fraction of the solvent ϕ_j . In addition, a binary adjustment parameter l_{ij} can be introduced, which is based on measurements. So far, this parameter is unknown. Figure 4 shows the results.

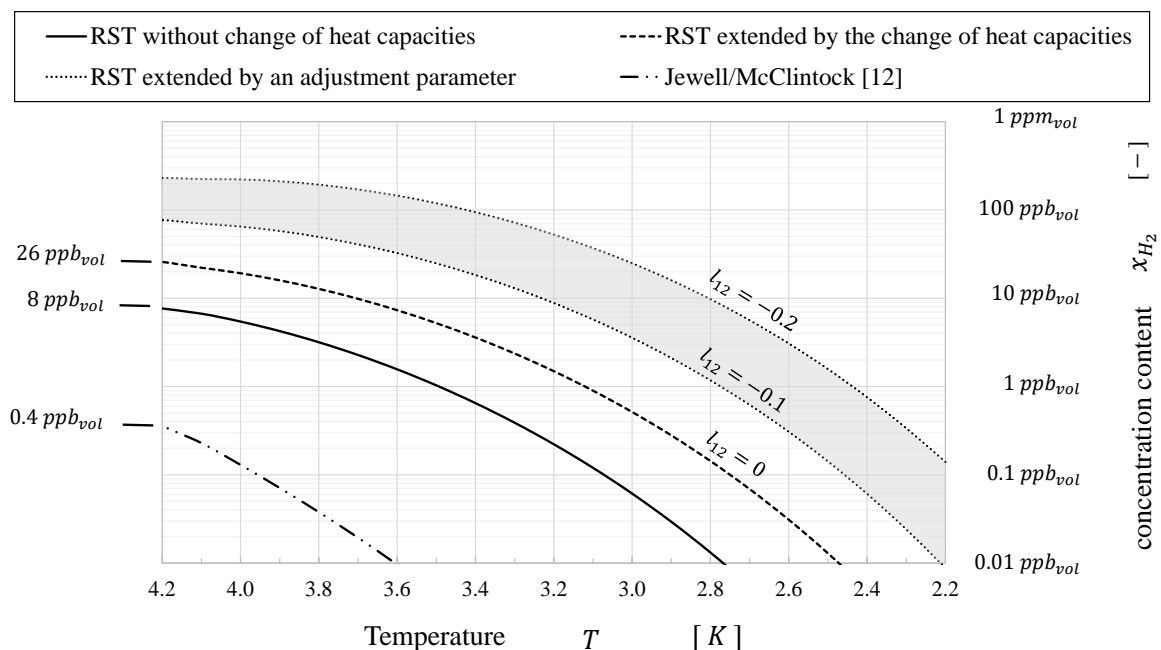


Figure 4. The diagram gives the results of the application of the Regular Solution Theory (RST). It shows the concentration content in the calculated equilibrium as a function of the liquid helium temperature range.

As expected, the equilibrium decreases with temperature reduction. The solid line describes the *ideal solubility* with the addition of the activity coefficient γ_{H_2} . At $T_{s,He} = 4.2$ K the calculation results in $x_{H_2} = 8$ ppb_{vol}. If the entire RST is applied, including activity coefficient and changes of the heat

capacity $\Delta c_{p,m,i}^{S \rightarrow L}$, the curve is corrected upwards by a factor of greater than 3 at the normal boiling point ($x_{H_2} = 26 \text{ ppb}_{vol}$). In the literature can be found the application of the RST by Jewell and McClintock from 1979 [12], which is presented for comparison. The differences are caused by a less precise parameterization of the model. In addition, the changes in heat capacity are not taken into account.

Values in the range of a few hundred ppb_{vol} were measured. To represent these values in the calculation, the binary adjustment parameter must be set in the range from $l_{ij} = -0.1$ to -0.2 . Experience has shown that these values for l_{ij} are one order of magnitude too high. A method has to be found which makes it possible to exclude the existence of crystalline hydrogen in liquid helium.

4. Gas chromatographic investigations on a small scale liquefier

In order to gain an understanding of the contamination processes in a liquefier, further gas chromatographic investigations were carried out. The university operates a liquefier that supplies critical contaminated liquid helium (TCF 20 from Linde with a capacity of 27 liters per hour and a stationary 2500 liter dewar). The system was sampled at two different operating points. To the one after a plant downtime of about 72 hours, on the other after a continuous plant operation of about 72 hours. Samples were taken from the buffer tank of the Claude process, from the gas phase of the stationary dewar, and from the liquid phase of the dewar. In Table 1 the results are shown.

Table 1. Results of gas chromatographic analyses on the helium liquefier (Linde-TFC20) of the Technische Universitaet Dresden (ppm_{vol} : volumetric parts per million, $\times 10^{-6}$).

	After plant downtime of $\approx 72h$	After plant operation of $\approx 72h$	After plant downtime of $\approx 72h$
	x_{H_2} (ppm_{vol})	x_{H_2} (ppm_{vol})	x_{H_2} (ppm_{vol})
Buffer tank	0.27	0.09	
Gas phase @ stationary dewar	12.1	0.05	0.02
Liquid phase @ stationary dewar	0.44	0.20	

With one exception, the contamination levels are in the range of a few tens to several hundred ppb_{vol} . The buffer tank is three times more contaminated after a longer downtime of the plant than after an extended operating time. In the liquid phase of the stationary dewar, the value is more than doubled. Different in the gas phase of the dewar, here a value three orders of magnitude larger was found (12.1 ppm_{vol}). To confirm this high value, the gas phase was sampled again after another downtime of the plant. The second measurement showed a value of 0.02 ppb_{vol} , so that it can be assumed that the gas phase was only that highly contaminated for a limited time.

From the measurements it can be seen that the internal purifying (particularly the 20 K carbon adsorber) is able to clean the helium to a large extent. The low values in the second column show this. From the high value it can be concluded that the warmed adsorber (shortly after the system has been stopped) releases the hydrogen. This then finds its way into the stationary dewar.

This hypothesis can help to understand why plants become more and more contaminated with time. The hydrogen is bound in the plants and remains. By substituting lost helium, additional hydrogen is introduced and accumulates until a critical limit is reached.

5. Use of a detection tool

The University of Zaragoza has developed a method for the rapid detection of critical quantities of hydrogen in liquid helium [3]. For this purpose, the blockage effect (see introduction) is reproduced in a particular manner. In order to achieve the effect, a flow resistor with an average channel diameter of $5\ \mu\text{m}$ was developed. To produce such a resistor, a focused ion beam is used to incorporate a corresponding channel into a very small sized copper platelet.

In order to test liquid helium, the resistor is immersed in the liquid by means of an assembly. It has to be pumped through the narrow channel by aid of a vacuum pump. The helium evaporates due to the resistance. If the helium is critically contaminated, the described blockage occurs within a few minutes. To detect this, it is necessary to measure the pressure of the pumped helium during the experiment. Two different cases are illustrated in Figure 5.

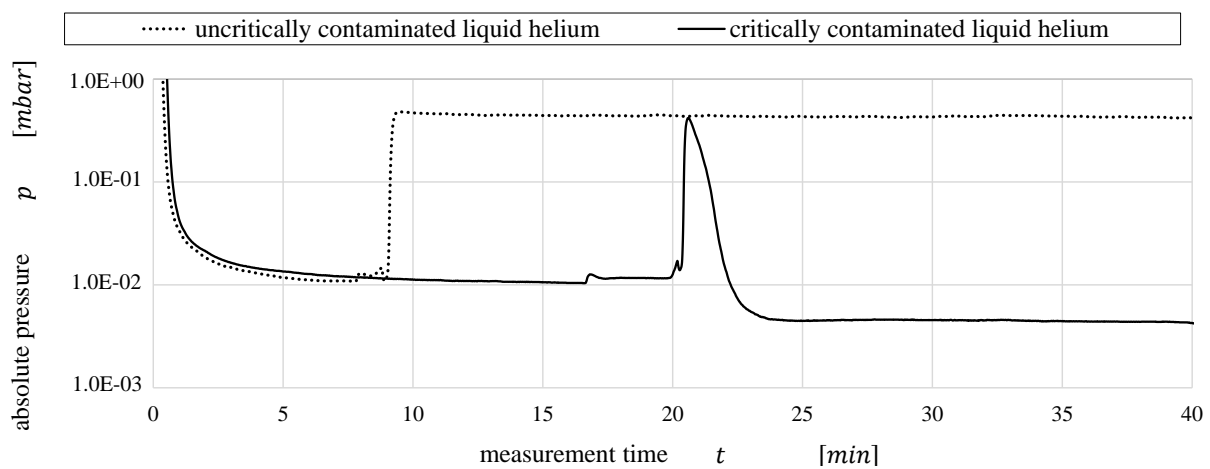


Figure 5. The dotted line indicates a low pressure loss due to the flow resistor. The solid line represents a large pressure loss due to a hydrogen blockage inside the resistor (measurement performed at Technische Universitaet Dresden).

The diagram shows the measurement of the pressure over the measurement time. In the beginning, both curves show the evacuating of the assembly. Gaseous helium flows through the resistor. The vacuum pump used achieves a negative pressure of $p \approx 1 \cdot 10^{-2}\ \text{mbar}$. At minute 8, the resistor is immersed in uncritically contaminated helium (dotted line). The higher viscosity of the liquid helium reduces the pressure loss. Now more helium flows through the resistor and a higher pressure is set behind. This pressure level of $p \approx 4.3 \cdot 10^{-1}\ \text{mbar}$ remains stable. This means that the resistor is not influenced and no blockage is occurred.

The second case describes the test with contaminated liquid helium (solid line). At minute 20, the resistor is immersed in the liquid helium. Again the pressure rises due to the reduced pressure loss caused by the lower viscosity. In difference to the first case, the formation of a hydrogen blockage begins at the next moment. The pressure loss increases and thus the measured pressure decreases. The negative pressure reaches $p \approx 4.4 \cdot 10^{-2}\ \text{mbar}$ after 3 minutes. This is the maximum negative pressure that the used vacuum pump can generate. It can be stated, the resistor is fully blocked by solid hydrogen.

6. Conclusion

The problem of the failure of helium flow cryostats to provide cooling capacity below 4.2 K was widely investigated. There is evidence that hydrogen impurities in liquid helium are responsible for this problem. Extremely low contents in the range of a few hundred ppb_{vol} in liquid helium were detected by measurement. These traces of hydrogen are more than enough to cause a blockage inside the cryostats. A calculation of the solubility equilibrium using the Regular Solution Theory shows that the equilibrium is probably even a factor lower. It can be assumed that besides dissolved hydrogen, solid crystalline hydrogen can also exist in liquid helium. Measurements in the helium reservoir show an inhomogeneous concentration distribution beyond the phase boundary over a wide temperature range in the gaseous helium phase. The hypothetical behavior of hydrogen in the cryogenic helium regime has been summarized using a macroscopic visualization model. Investigations carried out on a liquefier help to understand the contamination process. Furthermore, the function of a detection method of the University of Zaragoza was successfully demonstrated.

7. References

- [1] Ikeda H and Kondo Y 2015 Improvement of the Operational Settings of a Helium Purifier, Leading to a Higher Purity of the Recovered Gas *Physics Procedia* **67** 1153-1156
- [2] Decker L, Meier A and Wilhelm H 2014 Improvement of Linde Kryotechnik's internal purifier, *AIP Conference Proceedings* **1573** 957-961
- [3] Gabal M 2017 *New Cryocooler-Based Helium Liquefaction and Purification Techniques: from Recovered Gas to Ultra-Pure Liquid* (Zaragoza: Colección de estudios de física)
- [4] Gabal M, Arauzo A, Camón A, Castrillo M, Guerrero E, Lozano M P, Pina M P, Sesé J, Spagna S, Diederichs J, Rayner G, Sloan J, Galli F, van der Geest W, Haberstroh C, Dittmar N, Oca A, Grau F, Fernandes A and Rillo C 2016 Hydrogen-Free Liquid-Helium Recovery Plants: The Solution for Low-Temperature Flow Impedance Blocking *Physical Review Applied* **6** Iss. 2
- [5] Gabal M, Rillo C, Sesé J, Diederichs J, Rayner G and Spagna S 2016 Cryocooler-based Helium Recovery Plant for Applications requiring Gas or Liquid with Extreme Purity *Proc. 19th International Cryocooler Conference, San Diego* Iss. 523
- [6] Gabal M, Sesé J, Diederichs J, Rillo C and Spagna S 2017 The purity of liquid helium revisited, *Proc. 14th CRYOGENICS International Conference, Dresden, Germany* Paper ID 117
- [7] Gabal M, Sesé J, Rillo C and Spagna S 2018 "Clean" Liquid Helium *Superfluids and Superconductors* ed Roberto Zivieri (London: IntechOpen) chapter 4
- [8] Stewart R B and Roder H M 1964 Properties of Normal- and Parahydrogen *Technology and Uses of Liquid Hydrogen* ed Scott R B, Denton W H and Nicholls C M (New York: Pergamon) chapter 11
- [9] Lemmon E W, Bell I H, Huber M L and McLinden M O 2018 *NIST Standard Reference Database 23: Reference Fluid Thermodynamic and Transport Properties – REFPROP, Version 9.1* National Institute of Standards and Technology
- [10] Lüdecke D and Lüdecke C 2000 *Thermodynamik – Physikalisch chemische Grundlagen der thermischen Verfahrenstechnik, 1. Auflage* (Heidelberg: Springer-Verlag)
- [11] Poling B E, Prausnitz J M and O'Connell J P 2001 *The Properties of Gases and Liquids, 5th edition* (New York: McGraw-Hill)
- [12] Jewell C and McClintock P V E 1979 A note on the purity of liquid helium-4 *Cryogenics* **19** 682-683